

# NNMT contributes to high metastasis of triple negative breast cancer by enhancing PP2A/MEK/ERK/c-Jun/ABCA1 pathway mediated membrane fluidity

Yanzhong Wang<sup>a,b,c,1</sup>, Xi Zhou<sup>a,c,1</sup>, Yinjiao Lei<sup>a,c</sup>, Yadong Chu<sup>a,c,d</sup>, Xingtong Yu<sup>a,c</sup>, Qingchao Tong<sup>a,c</sup>, Tao Zhu<sup>e</sup>, Haitao Yu<sup>a,c</sup>, Sining Fang<sup>a,c</sup>, Guoli Li<sup>a,c</sup>, Linbo Wang<sup>f</sup>, Gavin Y. Wang<sup>g,h</sup>, Xinyou Xie<sup>a,b,c,\*\*</sup>, Jun Zhang<sup>a,b,c,\*</sup>

<sup>a</sup> Department of Clinical Laboratory, Sir Run Run Shaw Hospital, Zhejiang University School of Medicine, Hangzhou, Zhejiang, PR China

<sup>b</sup> Department of Clinical Laboratory, Xiasha Campus, Sir Run Run Shaw Hospital, Zhejiang University School of Medicine, Hangzhou, Zhejiang, PR China

<sup>c</sup> Key Laboratory of Precision Medicine in Diagnosis and Monitoring Research of Zhejiang Province, Hangzhou, Zhejiang, PR China

<sup>d</sup> Department of Clinical Laboratory, Zhejiang Armed Police Corps Hospital, Hangzhou, Zhejiang, PR China

<sup>e</sup> Department of Pathology, Sir Run Run Shaw Hospital, Zhejiang University School of Medicine, Hangzhou, Zhejiang, PR China

<sup>f</sup> Department of Surgical Oncology, Sir Run Run Shaw Hospital, Zhejiang University School of Medicine, Hangzhou, Zhejiang, PR China

<sup>g</sup> Department of Pathology and Laboratory Medicine, Medical University of South Carolina, Charleston, 29425, SC, USA

<sup>h</sup> Cancer Cell Biology Program of the Hollings Cancer Center, Medical University of South Carolina, Charleston, 29425, SC, USA

## ARTICLE INFO

### Keywords:

Cholesterol metabolism  
Epithelial-mesenchymal transition  
Methylation potential  
Lung metastasis  
Protein phosphatase

## ABSTRACT

Elucidating the mechanism for high metastasis capacity of triple negative breast cancers (TNBC) is crucial to improve treatment outcomes of TNBC. We have recently reported that nicotinamide N-methyltransferase (NNMT) is overexpressed in breast cancer, especially in TNBC, and predicts poor survival of patients undergoing chemotherapy. Here, we aimed to determine the function and mechanism of NNMT on metastasis of TNBC. Additionally, analysis of public datasets indicated that NNMT is involved in cholesterol metabolism. *In vitro*, NNMT overexpression promoted migration and invasion of TNBCs by reducing cholesterol levels in the cytoplasm and cell membrane. Mechanistically, NNMT activated MEK/ERK/c-Jun/ABCA1 pathway by repressing protein phosphatase 2A (PP2A) activity leading to cholesterol efflux and membrane fluidity enhancement, thereby promoting the epithelial-mesenchymal transition (EMT) of TNBCs. *In vivo*, the metastasis capacity of TNBCs was weakened by targeting NNMT. Collectively, our findings suggest a new molecular mechanism involving NNMT in metastasis and poor survival of TNBC mediated by PP2A and affecting cholesterol metabolism.

## 1. Introduction

Breast cancer has overtaken lung cancer as the most commonly diagnosed cancer worldwide, with about 2.26 million newly diagnosed cases and 680,000 deaths in 2020 reported by International Agency for Research on Cancer. Triple negative breast cancer (TNBC) is an aggressive and heterogeneous subtype of breast cancer that lacks

estrogen receptors, progesterone receptors and human epidermal growth factor receptor 2 expression, accounting for approximately 15–20% of all subtypes. Due to its high invasive nature, approximately 46% of patients with TNBC have distant metastasis and the mortality rate is 40% within the first 5 years after diagnosis [1]. Therefore, elucidating the mechanism contributing to high metastasis capacity of TNBC is very important to improve treatment outcomes and survival.

**Abbreviations:** 1-MNA, 1-methylnicotinamide; ANT, adjacent normal tissues; DFS, disease-free survival; CDH1, E-cadherin protein; CDH2, N-cadherin protein; EMT, epithelial-mesenchymal transition; GSEA, gene set enrichment analysis; IHC, immunohistochemistry analysis; NAM, nicotinamide; NNMT, nicotinamide N-methyltransferase; OS, overall survival; PP2A, protein phosphatase; TCGA, the Cancer Genome Atlas; TNBC, triple negative breast cancers.

\* Corresponding author. 3 East Qingchun Road, Hangzhou, Zhejiang, 310016, PR China.

\*\* co-corresponding author. 3 East Qingchun Road, Hangzhou, Zhejiang, 310016, PR China.

E-mail addresses: [scottxie@zju.edu.cn](mailto:scottxie@zju.edu.cn) (X. Xie), [jameszhang2000@zju.edu.cn](mailto:jameszhang2000@zju.edu.cn) (J. Zhang).

<sup>1</sup> These authors contributed equally to this work.

<https://doi.org/10.1016/j.canlet.2022.215884>

Received 7 March 2022; Received in revised form 12 August 2022; Accepted 12 August 2022

Available online 19 August 2022

0304-3835/© 2022 The Authors. Published by Elsevier B.V. This is an open access article under the CC BY-NC-ND license (<http://creativecommons.org/licenses/by-nc-nd/4.0/>).

The dysregulation of cellular metabolism and activated invasion and metastasis are two hallmarks of cancer [2]. The cancer metabolism depends on alterations of key metabolic pathways and has a profound effect on the expression of oncogenes and tumor suppressor genes, which are involved in the regulation of proliferation, apoptosis, autophagy and metastasis in cancer.

Nicotinamide N-methyltransferase (NNMT) is a cytosolic enzyme that catalyzes the transfer of the methyl units from S-adenosyl-L-methionine (SAM) to nicotinamide (NAM), producing the stable metabolic product 1-methylnicotinamide (1-MNA) [3]. As a result, NNMT expression controls the methylation potential of cancer cells, leading to an altered epigenetic state that includes hypomethylated histones and other cancer-related proteins, such as histone H3K4, H3K9, H3K27, H4K20 and tumor suppressor PP2A [3]. Based on this basic function, the overexpression of NNMT in various types of cancer including breast cancer [3–16] impairs proliferation, apoptosis, autophagy, nutrient metabolism and metastasis [3,9,17–19], thereby affecting the treatment and survival of patients with liver, prostate, gastric and pancreatic cancer [11,14–16]. Recently, we have reported that high NNMT expression in breast cancer can inhibit apoptosis and enhance chemotherapy resistance, resulting in poor survival [20,21]. Meanwhile, our preliminary findings suggest that 66.7% of TNBC patients with high NNMT expression in tumor tissues was higher than those in other subtypes [21].

In this study, we aimed to expand our observation cohort to assess NNMT expression in tumor tissues and associated lymph nodes and study their metastasis and survival. We further constructed TNBC cell line models and assessed the mechanism towards enhanced metastasis. We believe that this study would provide a promising therapeutic strategy to overcome high metastasis of TNBC.

## 2. Materials and methods

### 2.1. Cells, antibodies and reagents

The human breast cancer cell lines SK-BR-3, MCF7, MDA-MB-468, MDA-MB-231, BT-549, HCC1937 and T47D were purchased from American Type Culture Collection (ATCC, USA). SK-BR-3, MCF7, MDA-MB-468 and MDA-MB-231 cells were cultured in DMEM (Gibco). HCC1937 cells were grown in RPMI 1640 medium (Gibco). BT-549 cells were cultured in RPMI 1640 medium containing 0.023 U/mL insulin. All mediums were supplemented with 10% fetal bovine serum (Gibco), 100 U/mL of penicillin (Sigma-Aldrich) and 100 µg/mL of streptomycin (Sigma-Aldrich). The cells were maintained at 37 °C in a humidified 5% CO<sub>2</sub> incubator.

The anti-SREBF2 (7119-SP) antibody was purchased from R&D Systems, anti-HMGCR (ab174830), anti-LDLR (ab52818), anti-ABCA1 (ab18180), anti-c-Jun (ab31419), anti-RACK1 (ab62735) and anti-PCNA (ab18197) from Abcam, EMT antibody sampler kit (9782), anti-PP2A (2038S) anti-MEK (9122S), anti-p-MEK (9154S), anti-ERK (4695S), anti-p-ERK (4370S), anti-AKT (4691S), anti-p-AKT (4060S) and anti-β-actin (8457) from Cell Signaling Technology and anti-methyl-PP2A (sc-81603), anti-JNK (sc-7345) and anti-p-JNK (6245) from Santa Cruz biotechnology. Anti-NNMT(1E7) was obtained through the hybridoma technique as previously described [20]. Goat anti-mouse (FD0142) and goat anti-rabbit (FD0128) HRP-conjugated antibodies were purchased from Hangzhou FUDE Biological Technology.

Filipin (F4767), cholesterol (C3045), PD98059 (19–143), Mevastatin (M2537) and 1-MNA (1005-24-9) from Sigma Aldrich, Dil-C16 (D384) from Thermo Fisher Scientific and lipoprotein deficient serum (BT-907) from Bovine were purchased.

### 2.2. Patients' characteristics and immunohistochemistry analysis

This study was approved by the Human Research Ethics Committee of Sir Run Run Shaw Hospital (Permit Number: 20180601–006). The

diagnoses of 309 patients with breast cancer were confirmed by post-operative pathological results from January 1, 2009 to Dec 31, 2017 at Sir Run Run Shaw Hospital (Hangzhou, China). The clinical characteristics of these patients were extracted from their medical record, including age, TNM stage (tumor diameter, lymph node metastasis and distant metastasis), ER, Her-2, and PR according to the guideline for breast cancer of Chinese society of clinical oncology (Version 2020). These patients were followed up, and the overall survival (OS) was calculated from the date of surgical treatment to the date of death or last follow-up.

Formalin-fixed, paraffin-embedded tissue sections (4 µm) were deparaffinized, rehydrated and induced with 0.01 M citrate buffer pH 6.0 and microwave heated for half an hour. Then, the sections were treated with 1% H<sub>2</sub>O<sub>2</sub> for 5 min and normal goat serum at room temperature for 10 min. The sections were then incubated with mouse monoclonal anti-human NNMT antibody (1E7, dilution 1:1400) for 40 min and with goat anti-mouse secondary antibody for 30 min. Sections were developed with diaminobenzidine and then counterstained with hematoxylin. Finally, the images of immunohistochemistry (IHC) were captured by digital slide scanning system (KF-PRO-005, Ningbo Jiangfeng Biological Information Technology Co. Ltd.). The expression level of NNMT was evaluated by two pathologists, who were blinded to clinical information. The final staining score was determined by percentage of positive cells and respective intensity scores. The cut-off value of NNMT expression for breast cancer determination was 40 by receiver operating characteristic (ROC) curve using GraphPad Prism 7.0 software program.

### 2.3. Public dataset analysis

We analyzed the expression and prognostic value of NNMT in TNBC by the Cancer Genome Atlas (TCGA), Metabric dataset, BreastMark and clinical microarray datasets, respectively. We integrated the patients with TNBC in six cohorts (TCGA-TNBC, GSE14017, GSE76124, GSE46141, GSE56493 and METABRIC) from the repository of GEO, METABRIC and TCGA according to the clinical phenotype, to perform the GSEA method to explore the NNMT related metabolism pathways among these patients. The patients were divided into two groups by using the median expression values of NNMT in each cohort. The detailed clinical data of 1992 patients with breast cancer were obtained from Metabric dataset (EGAS00000000083), containing 320 TNBC and 1672 non-TNBC.

### 2.4. Lentiviral infection and siRNA transfection

Cells were seeded ( $2 \times 10^5$  cells/well) in six-well plates overnight and co-cultured with lentivirus containing shRNA targeting human NNMT gene from GeneChem Co. Ltd (Shanghai, China) as reported previously [21] or transfected with c-Jun siRNA (20 nM), ABCA1 siRNA (20 nM) or control siRNA (20 nM, sc-37007) in opti-MEM, using Lipofectamine 3000 (Thermo Fisher Scientific) for 12 h. The siRNA sequences targeting c-Jun and ABCA1 were listed in [Supplementary Table S1](#). Further, cells were incubated in fresh medium.

### 2.5. Construction of NNMT mutant and overexpression cell lines with pLenti-Pur plasmid transfection

The human NNMT mutation (Y20) has more than 90% loss of its N-methyl transferase activity [19]. HEK293T cells were transfected with 10 µg pLenti-Pur-NNMT (NCBI Reference Sequence: NM\_00132045.1) or pLenti-Pur-NNMT-Y20 or pLenti-Pur plasmid (Vigenebio, China) as control using Lipofectamine 3000 reagent. Viral supernatant was harvested from HEK 293T cells after 48 h and filtered using 0.45 µm filter (Millipore). HCC1937 cells were incubated with viral supernatant for 24 h and the supernatant was replaced with fresh medium. After infection, cells were selected with puromycin (1 µM) for 5 days.

## 2.6. Wound healing assay

Cells were grown to 100% confluency in 6-well tissue culture plates and then incubated in starvation media (0.1% FBS) for 12 h. The monolayers cells were scraped with sterile 200  $\mu$ L pipette tips. Images of wounded cells were captured at 6 migration points at the beginning and after 18 h of the assay. The gap distances at 0 h and 18 h after wounding were measured and migration efficiency was calculated as: (gap area at 0 h - gap area at 18 h)/(gap area at 0 h).

## 2.7. Invasion and migration assay

Cells were starved in low serum (0.1% FBS) medium for 12 h and then trypsinized. Further,  $2 \times 10^4$  cells were resuspended in 200  $\mu$ L starvation medium (0.1% FBS) and loaded in the upper chamber of Corning clear Transwell 24-well permeable supports in a 24-well plate. The chamber with Matrigel (Corning) was for invasion assay and the chamber without Matrigel (Corning) was for migration assay. The bottom chamber was filled with complete growth medium. After 8 h of incubation at 37 °C and 5% CO<sub>2</sub>, unigrated cells on the upper surface of the chamber were carefully removed using a cotton bud. The migrated cells were fixed with 100% methanol for 15 min and washed with PBS twice at room temperature. The cells were then stained with 0.1% crystal violet dye, imaged at 40 $\times$  magnification using Carl Zeiss Microscopy and 5 random visual fields were counted.

## 2.8. Quantitation of cholesterol

Total cellular cholesterol concentration was quantified using Amplex® Red Cholesterol Assay (Thermo Fisher Scientific). The cells were lysed in 0.5% Triton X-100 and then incubated for 30 min with agitation before addition of the reaction mix (cholesterol oxidase, HRP, etc). The samples were incubated for 30 min at 37 °C in dark and measured using fluorescence microplate reader with excitation at 530 nm and emission detection at 590 nm.

## 2.9. Filipin staining of cholesterol

Cells were grown in chambers at a density of  $4 \times 10^4$  cells/well. After treatment, cells were rinsed with PBS, fixed with 4% paraformaldehyde for 15 min and then blocked with 1% BSA in PBS for 1 h at room temperature. Then, cells were washed with PBS and stained with 50  $\mu$ g/mL filipin in the dark for 2 h at room temperature. The filipin signals (intracellular and on the cell membrane) of 20 random stained cells were analyzed with a Zeiss LSM 880 confocal microscope using an excitatory wavelength of 405 nm. In each experiment, images were acquired at identical laser output, gain, and offset.

## 2.10. RNA isolation and real time Quantitative PCR

Total RNA was isolated using TRIzol reagent (Invitrogen) according to the manufacturer's protocol. For mRNA quantification, cDNA was synthesized using HiFiscript cDNA Synthesis kit (Comwin Biotech), following the manufacturer's protocol. The sequences of all specific primers were listed in [Supplementary Table S2](#). Quantitative real-time PCR (qRT-PCR) analysis was performed in triplicate using the NovoStart® SYBR qPCR SuperMix Plus (Novoprotein). The mRNA levels were normalized to that of  $\beta$ -actin.

## 2.11. Western blot analysis

Cells were washed with cold PBS, homogenized in RIPA buffer (Beyotime biotechnology) containing protease inhibitors (Roche), and lysed for 30 min at 4 °C followed by centrifugation at 12000 rpm for 15 min. The nuclear lysate was prepared for c-Jun protein detection using the Nuclear Extract Kit (Abcam). Protein concentration were measured

using a BCA Protein Assay Kit (Beyotime biotechnology). Protein was analyzed using SDS-polyacrylamide gel electrophoresis and transferred to Immobilon P Transfer Membrane (Millipore) blocked with 5% milk in TBST for 1 h at room temperature. The membrane was incubated with the antibody overnight at 4 °C and then washed with Tris-buffered saline containing Tween 20, and incubated with horseradish peroxidase-conjugated secondary antibody for 1 h at room temperature. Followed by washing in TBST, the signals were visualized using the chemiluminescence detection reagents, imaged using a ChemiDoc Touch Imaging system and analyzed using Image lab software (Bio-Rad).

## 2.12. Quantification of 1-MNA and SAM by LC-MS/MS

SAM and 1-MNA were measured using LC-MS/MS with AB SCIEX Triple Quad™ 4500MD mass spectrometry system. Briefly, 250  $\mu$ L of 1% zinc sulfate solution with stable isotope labelled internal standard (N-MNA-d4) was added into 50  $\mu$ L cell samples or a series of concentration standards (1-MNA and SAM). After shaking at 400 rpm for 30 min and samples were centrifuged at 14000 rpm for 20 min, the supernatant was transferred to glass vials for LC-MS/MS. Liquid chromatography separation was performed by injecting 5  $\mu$ L sample into the Eclipse XDB-C18 column (4.6  $\times$  150 mm, 5  $\mu$ m; Agilent) connected to Jasper™ (SCIEX) LC system. The isocratic mobile phase, a mixture of 0.1% formic acid and methanol mixture (v/v) was filtered through a 0.22  $\mu$ m membrane filter (Millipore) and then degassed ultrasonically for 15 min to be delivered at a flow rate of 1 mL/min into the mass spectrometer electrospray ionization (ESI) chamber. The retention times of 1-MNA, SAM and N-MNA-d4 were 1.31, 1.20 and 1.65 min, respectively. The final concentration is quantified based on the protein of the cell.

## 2.13. Membrane fluidity assay by fluorescence recovery after photobleaching (FRAP)

Cells were cultured in the Lab-TEK II chamber slide (Thermo Fisher) for 12 h and then incubated in 1  $\mu$ g/mL Dil-C16 solution for 60 s at room temperature. The chamber slide was placed on the pre-heated stage (37 °C) imaging chamber of Zeiss LSM 880 confocal microscope. With a 63 $\times$  oil objective, a small area (1  $\times$  1  $\mu$ m) of the membrane was photobleached by 100% laser (561 nm) excitation. The fluorescence intensity of pre-bleach and post-bleach was recorded every 10 s over a period of 3 min. The fluorescence intensity was normalized at each time point by subtracting the background values to remove experimental noise and then generate the fluorescence recovery curve.

## 2.14. Luciferase assays

$1 \times 10^5$  cells were seeded on a 24-well plate and grew to 80–90% confluency. Cells were transfected with 50 ng renilla luciferase control vector pRL, 225 ng control pCMV6 plasmid and 225 ng ABCA1 promoter luciferase reporter (Full-length) or 50 ng renilla luciferase control, 225 ng wt c-Jun pCMV6 plasmid and 225 ng ABCA1 promoter luciferase reporter (Full-length) using Lipofectamine 3000. After 48 h, cell lysates were detected for Firefly and Renilla luciferase by using dual-luciferase assay (Yeasen) on a white 96 plate reader (Costar). Firefly luciferase values were normalized to Renilla luciferase as the relative luciferase values. The promoter luciferase reporter (Full-length) was a gift from David Mu (Addgene plasmid # 86442; <http://n2t.net/addgene:86442>; RRID: Addgene\_86442).

## 2.15. Metastatic animal models

The animal experiment was approved by the Institutional Animal Care and Use Committee of Sir Run Run Shaw Hospital. All procedures were performed in accordance with the ethical guidelines of the Declaration of Helsinki. Five weeks old female SCID mice were obtained to construct the metastatic model. MDA-MB-231/shNC, MDA-MB-231/

shNNMT-1 cells ( $1 \times 10^6$ ,  $1 \times 10^5$ ,  $1 \times 10^4$ ) and HCC1937/Vector, HCC1937/NNMT<sup>OE</sup>, HCC1937/NNMT<sup>Y20</sup> cells ( $5 \times 10^5$ ) were respectively suspended in 100  $\mu$ L PBS, respectively and injected into the lateral tail vein of mice (n = 6 for each group). Eight weeks after injection, the animals were killed by cervical dislocation. For metastasis quantification, the lungs were excised and embedded in paraffin. To examine lung metastases, embedded lungs were sectioned and stained with H&E and Immunohistochemistry analysis (IHC). The number of metastatic foci were counted independently by three investigators. NNMT, ABCA1 and c-Jun expressions were also analyzed by IHC.

2.16. Statistical analysis

Statistical analysis was performed using SPSS 22.0 (SPSS Inc., Chicago, IL). For our clinical data, the relationships between NNMT expression and clinicopathological characteristics were analyzed using Pearson's  $\chi^2$  test. Survival analysis was performed using Kaplan-Meier

(KM) method and compared using log-rank test. In *in vitro* and *in vivo* experiments, the statistical significance between groups was calculated by two-tailed Student's test. The *in vitro* experiments were performed independently at three times. Significance values are \*P < 0.05, \*\*P < 0.01, \*\*\*P < 0.001, \*\*\*\*P < 0.0001.

3. Results

3.1. Higher expression of NNMT in TNBC is associated with metastasis and poor survival

We reported NNMT to be highly expressed in breast cancer [21]. In this study, we included 221 patients with non-TNBC and 88 with TNBC. The comprehensive IHC scores of NNMT in tumor tissues, especially in TNBC, are significantly higher than those in adjacent normal tissues (ANT) (Fig. 1a and b), which were consistent with our previous report [21]. The percentage of high NNMT expression in TNBC was 69.3%

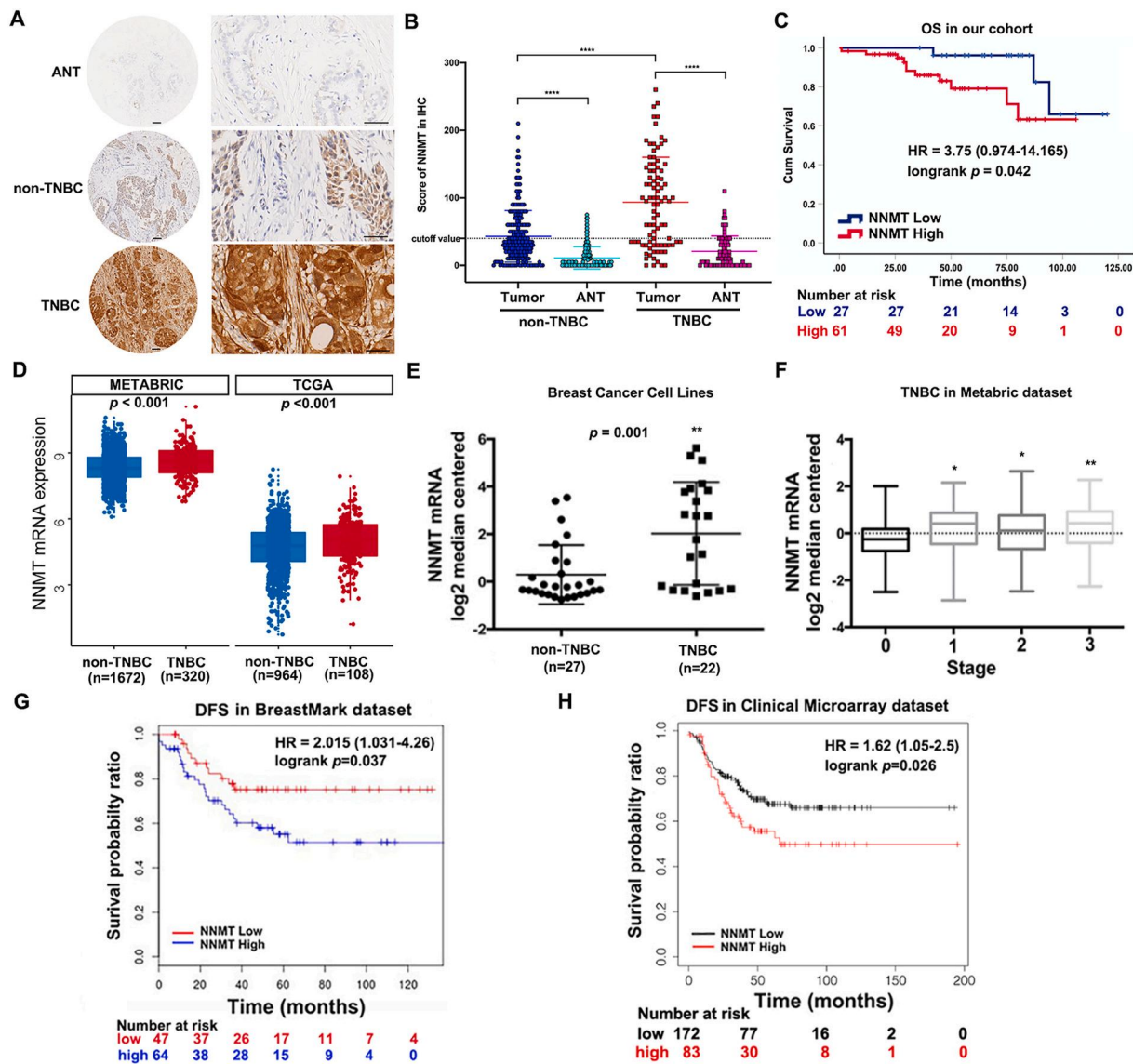


Fig. 1. NNMT is highly expressed in TNBC and associated with high metastasis and poor survival. (A) Representative image of NNMT staining in ANT, non-TNBC and TNBC (Scale bar: 100  $\mu$ m). (B) IHC scores of NNMT expression in tumor tissues and adjacent normal tissues of non-TNBC and TNBC. (C) OS analysis for 88 TNBC patients by NNMT protein expression. (D) NNMT mRNA levels in TNBC and non-TNBC patients' tumor tissues from Metabric and TCGA datasets. (E) NNMT mRNA levels in 22 TNBC and 27 non-TNBC cell lines. (F) NNMT mRNA levels in four tumor stages of TNBC in Metabric dataset. (G) DFS analysis for TNBC patients from BreastMark dataset by NNMT mRNA level. (H) DFS analysis for TNBC patients from Clinical Microarray dataset by NNMT mRNA level. (\*P < 0.05, \*\*P < 0.01, \*\*\*P < 0.001, \*\*\*\*P < 0.0001).

**Table 1**

Association of NNMT expression with clinicopathological characteristics in 88 TNBC patients.

Patients' characteristics	n	NNMT <sup>h</sup> (n, %)	Pearson's $\chi^2$	P
<b>Total</b>	88	61(69.3)		
<b>Age (years)</b>			0.139	0.709
≤52	45	32(71.1)		
>52	43	29(67.4)		
<b>Differentiation</b>			0.413	0.813
Low	9	7(77.8)		
Moderate	14	10(71.4)		
High	65	44(67.7)		
<b>TNM</b>			7.699	0.006
I + II	60	36(60.0)		
III + IV	28	25(89.3)		
<b>Primary tumor size</b>			0.337	0.561
T1+T2	79	54(68.4)		
T3+T4	9	7(77.8)		
<b>Lymph node metastasis</b>			4.555	0.033
N0+N1	65	41(63.1)		
N2+N3	23	20(87.0)		
<b>Distant metastasis</b>			3.366	0.067
M0	81	54(66.7)		
M1	7	7(100.0)		

NNMT<sup>h</sup>: NNMT high expression.

(Table 1), which was significantly higher than that in non-TNBC (37.1%) (Supplementary Table 3). Then, we analyzed the relationship between NNMT expression and clinicopathological characteristics in TNBC. The results showed that higher NNMT expression was significantly correlated with poorer TNM ( $P = 0.006$ ), higher lymph node metastasis ( $P = 0.033$ ) and shorter OS ( $P = 0.042$ ) and seven patients with distant metastasis all had higher NNMT expression ( $P = 0.067$ ) (Table 1 and Fig. 1c) in TNBC. Then, we performed a parallel analysis in different

public datasets. Consistent with our cohort result, NNMT mRNA levels of TNBC tumors are remarkably higher than those of non-TNBC (Fig. 1d) both in TCGA and Metabric datasets. Meanwhile, NNMT mRNA levels were significantly higher in TNBC cell lines than those in non-TNBC cell lines by the expression chip data of 49 breast cancer cell lines reported by C.F. Roff et al. [22] (Fig. 1e). In addition, high NNMT mRNA level is correlated with poor tumor stage in Metabric dataset (Fig. 1f) and shorter disease-free survival (DFS) in BreastMark mRNA dataset ( $P = 0.037$ ; Fig. 1g) and Clinical Microarray dataset ( $P = 0.026$ ; Fig. 1h). Taken together, our cohort data and public datasets reveal that NNMT is particularly highly expressed in TNBC and is associated with high metastasis and poor survival.

### 3.2. NNMT promotes cell migration and invasion of TNBC cells

To determine the function of NNMT in metastasis of TNBC *in vitro*, we first screened TNBC cell lines in our lab for NNMT expression. Non-TNBC cell lines (SK-BR-3, MCF7 and T47D) have low NNMT expression, whereas three TNBC cell lines have high NNMT expression, including BT-549, MDA-MB-468 and MDA-MB-231 cells. And, only HCC1937 cells have low NNMT expression in TNBC (Supplementary Figs. 1a, b, c), which is consistent with the data reported by C.F. Roff et al. Therefore, we chose MDA-MB-231, BT-549 and HCC1937 cells to construct cell models with different NNMT expression levels. We retrovirally established overexpression of NNMT or NNMT mutation (Y20) in HCC1937 cells and NNMT downregulation in MDA-MB-231 and BT-549 cells, while HCC1937/Vector, MDA-MB-231/shNC and BT-549/shNC cells respectively were used as control groups (Supplementary Figs. 1d, e, f).

The wound healing assay showed that the migration efficiency was significantly decreased after NNMT downregulation in both MDA-MB-

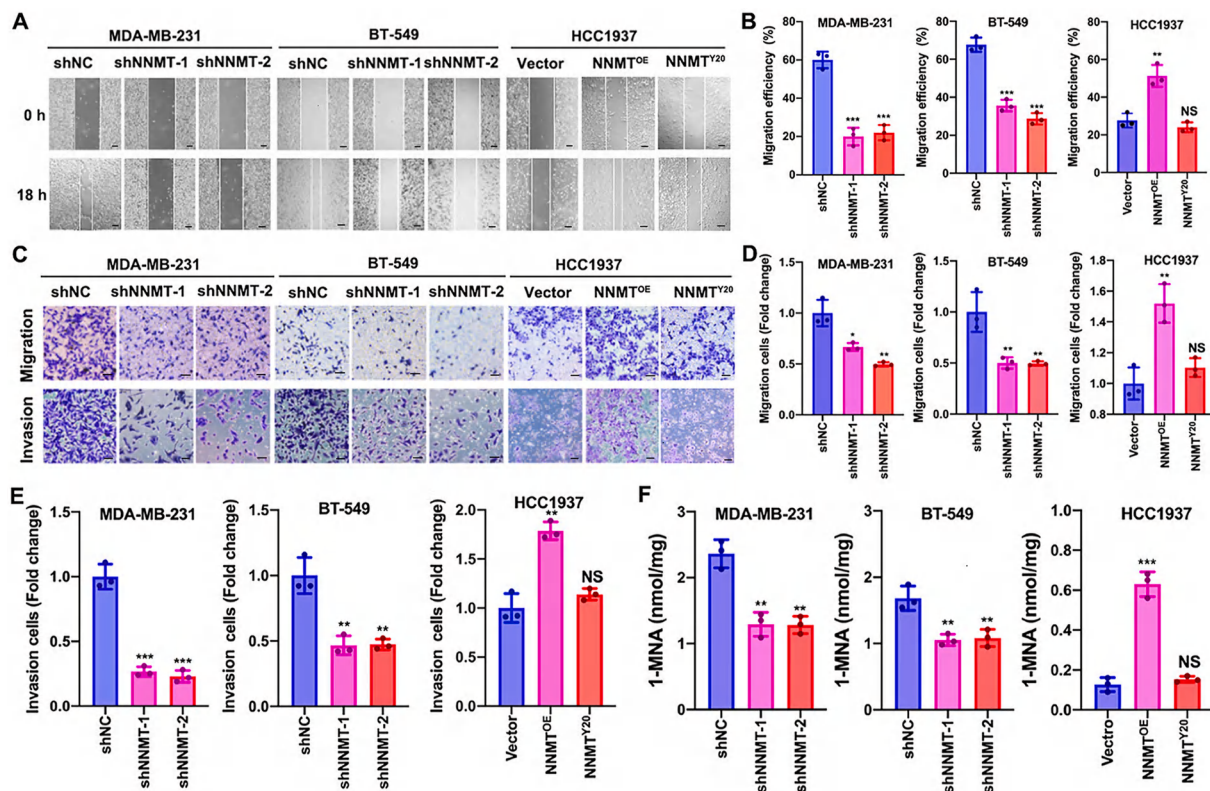


**Fig. 2.** NNMT promotes cell migration and invasion of TNBC cells. (A) Representative results of wound healing assay (Scale bar: 100  $\mu$ m). (B) Quantified migration efficiency of wound healing assay. (C) Representative results of migration and invasion assays (Scale bar: 100  $\mu$ m). (D) Fold change of migration cell numbers. (E) Fold change of invasion cell numbers. (F) Intracellular 1-MNA levels by LC-MS/MS. Each experiment was repeated three times. Data are expressed as mean  $\pm$  SEM. (\* $P < 0.05$ , \*\* $P < 0.01$ , \*\*\* $P < 0.001$ , NS = Not significant).

231 and BT-549 cell models, whereas it was significantly increased after NNMT overexpression in HCC1937 cell models (Fig. 2a and b). The migration and invasion assay showed the same trend. The migration and invasion cell numbers with NNMT downregulation were both significantly decreased, whereas they were remarkably increased after NNMT overexpression (Fig. 2c, d, e). These results indicated that NNMT

promotes migration and invasion capacities of TNBC cells. SAM is the methyl source for numerous reactions of methyl catalysis within cells and represents the methylation potential to some extent. In our cell models, the SAM level was increased with NNMT knockdown in MDA-MB-231 and BT-549 cells, whereas it was decreased with NNMT overexpression in HCC1937 cells (Supplementary Fig. 2). This result

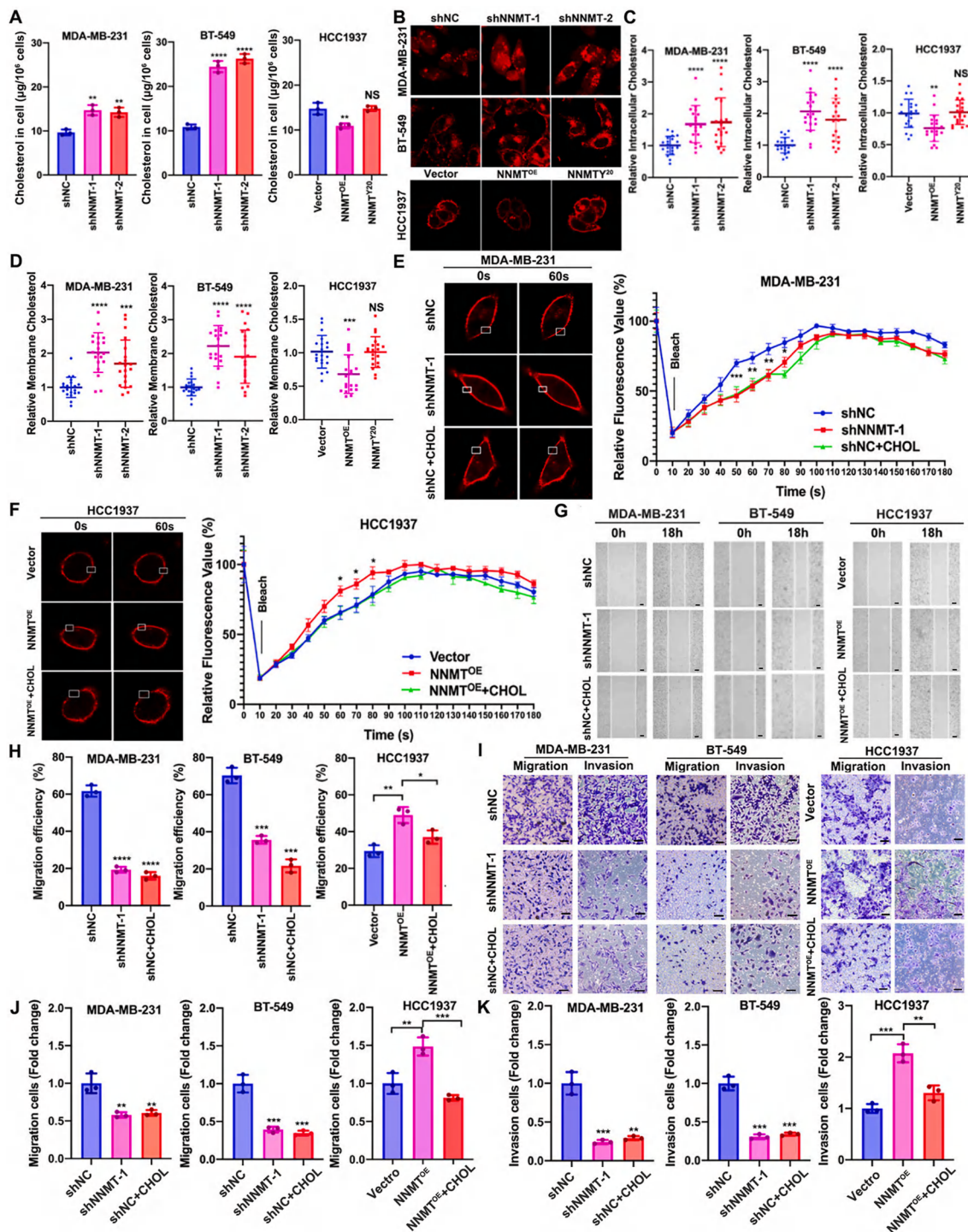


**Fig. 3.** NNMT promotes migration and invasion by reducing cholesterol in TNBC cells. (A) Intracellular cholesterol levels by Amplex® Red Cholesterol Assay. (B) Representative results of filipin staining. The relative cholesterol levels in cell (C) and on cell membrane (D) by filipin staining. (E, F) Representative results of DiI-C16 staining and the fluorescence recovery record using confocal microscope. The representative results (G) and migration efficiency (H) of wound healing assay with cholesterol treatment. (I) Representative results of migration and invasion assays with cholesterol treatment (Scale bar: 100 μm). The fold changes of migration (J) and invasion (K) cell number with cholesterol treatment. Each experiment was repeated three times. Data are expressed as mean ± SEM. (\**P* < 0.05, \*\**P* < 0.01, \*\*\**P* < 0.001, \*\*\*\**P* < 0.0001, NS = Not significant).

indicated that NNMT depletes SAM through catalytic function, thereby reducing the methylation potential of breast cancer cells, which is consistent with the previous report [3]. 1-MNA is only produced by the methyl transfer catalysis of NNMT, and the Y20 mutant is to make NNMT protein lose its catalytic function. The NNMT downregulation reduced intracellular 1-MNA, while NNMT overexpression increased intracellular 1-MNA, but there was no significant difference between HCC1937/NNMT<sup>Y20</sup> and HCC1937/Vector (Fig. 2f). However, it is worth noting that the NNMT<sup>Y20</sup> mutant did not have the promotion effect of wild type NNMT overexpression on migration and invasion (Fig. 2a–e), which suggested that NNMT may promote migration and invasion in TNBC by its methyl transfer function.

### 3.3. NNMT promotes cell migration and invasion through reducing cholesterol level to enhance membrane fluidity in TNBC cells

To explore the mechanism of NNMT on migration and invasion in TNBC cells, we examined the cholesterol in cell and on cell membrane, which is an essential structural component of cellular membranes, directly affecting membrane fluidity and EMT [23]. The intracellular cholesterol was significantly increased after NNMT downregulation both by Amplex® Red cholesterol assay and filipin staining, whereas it was decreased after NNMT overexpression (Fig. 3a, b, c). The cholesterol on cell membrane had the same trend in filipin staining (Fig. 3b, d). Interestingly, NNMT<sup>Y20</sup> mutant did not have the effect of high NNMT expression on cholesterol (Fig. 3a–d), indicating that NNMT decreases cholesterol level both in cell and on membrane in TNBC cells by its

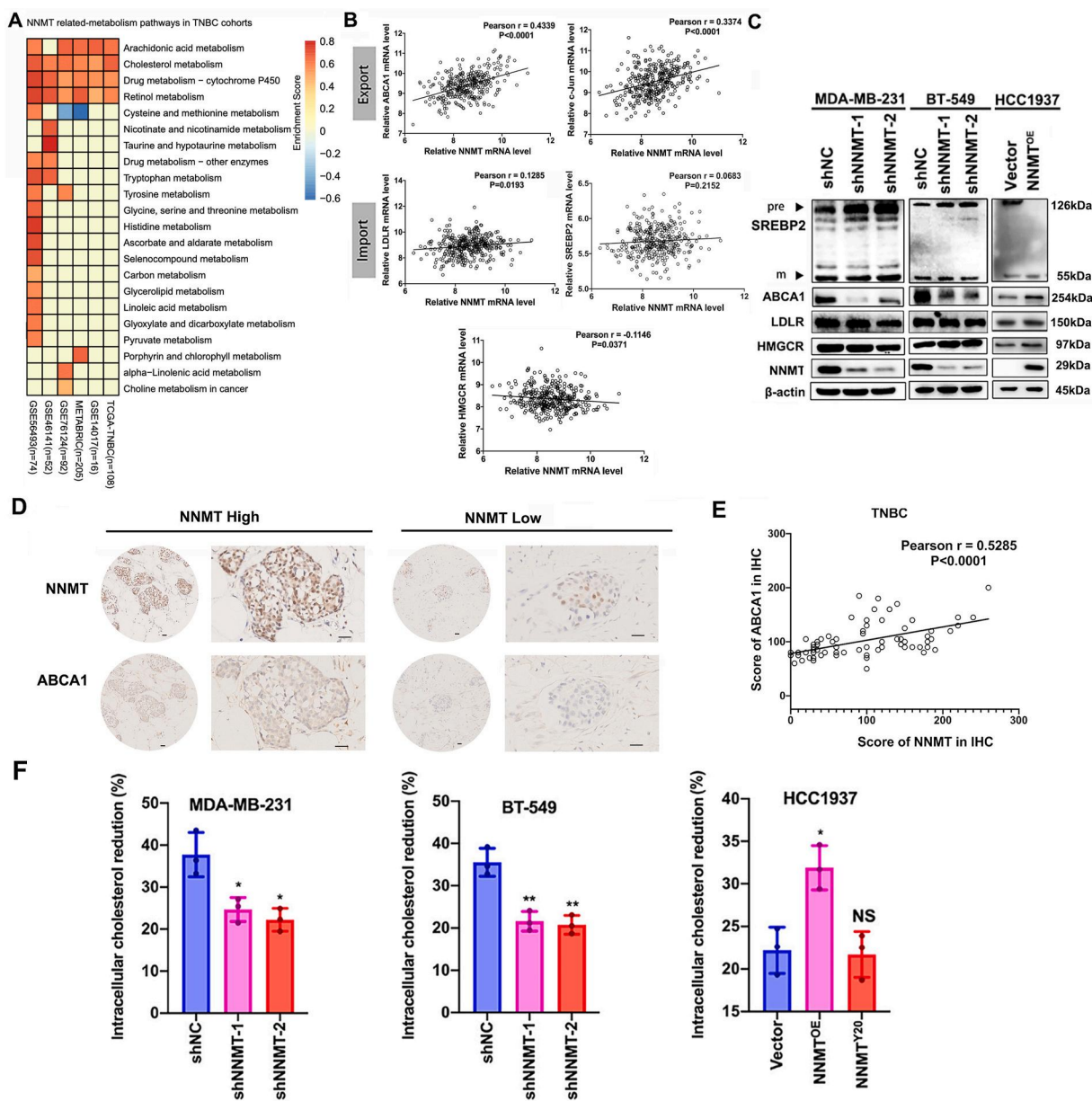


**Fig. 4.** NNMT promotes ABCA1 expression to enhance cholesterol efflux. (A) The NNMT related metabolism pathways among the TNBC patients were explored in six cohorts (TCGA-TNBC, GSE14017, GSE76124, GSE46141, GSE56493 and METABRIC) by GSEA. (B) Relationship between the mRNA levels of ABCA1, c-Jun, LDLR, SREBP2, HMGCR and NNMT in TNBC from Metabric dataset. (C) Representative results of cholesterol metabolism related protein levels. (D) Representative IHC results of NNMT and ABCA1 proteins in TNBC tumors (Scale bar: 100 μm). (E) Relationship between the protein levels of NNMT and ABCA1 from (D). (F) Intracellular cholesterol reduction percentages after cholesterol synthesis and absorption inhibition. Each experiment was repeated three times. Data are expressed as mean ± SEM. (\*P < 0.05, \*\*P < 0.01, NS = not significant).

methyl transfer function.

Further, we detected the membrane fluidity change in our cell models. The fluorescence in MDA-MB-231/shNNMT-1 cells displayed slower recovery than that in MDA-MB-231/shNC cells, whereas it recovered faster in HCC1937/NNMT<sup>OE</sup> cells than that in HCC1937/Vector cells. Moreover, cholesterol treatment significantly slowed the fluorescence recovery (Fig. 3e and f). These results indicated that NNMT expression increases membrane fluidity by reducing cholesterol in TNBC cells. Moreover, cholesterol treatment interfered with the promotion effect of NNMT expression on migration and invasion (Fig. 3g–k), which further demonstrated that NNMT expression promotes cell migration and invasion by reducing cholesterol to enhance membrane fluidity in TNBC cells.

### 3.4. NNMT promotes ABCA1 expression to enhance cholesterol efflux leading to cholesterol reduction in cell and on membrane of TNBC cells

To determine the association between NNMT and cholesterol metabolism in breast cancer, we performed the gene set enrichment analysis (GSEA) in six cohorts (TCGA, GSE14017, GSE76124, GES46141, GSE56493 and Metabric). GSEA results showed that the cholesterol metabolism pathway had higher enrichment score in all high NNMT mRNA expression groups than that in low NNMT groups (truncated by the median value) (Fig. 4a). We further explored the function of NNMT on cholesterol metabolism of TNBC, which is regulated by cholesterol uptake, synthesis and efflux. In the mRNA data from Metabric dataset, the mRNA levels of cholesterol efflux channel ABCA1 and the potential transcription factor c-Jun [24] in the TNBC tumors are significantly positively correlated with NNMT mRNA expression, as well as LDLR that regulates the uptake of cholesterol. However, SREBF2 and HMGCR which regulate the synthesis of cholesterol have no significant correlation with NNMT (Fig. 4b). In our cell models, MDA-MB-231 and BT-549 cells with NNMT downregulation had lower ABCA1 protein, whereas HMGCR, LDLR and mature SREBF2 proteins were not altered. In contrast, compared with HCC1937 control cells, HCC1937 cells with NNMT overexpression displayed higher ABCA1 protein, whereas HMGCR, mature SREBF2 and LDLR proteins were not altered (Fig. 4c). The mRNA result is entirely consistent with the protein (Supplementary Figs. 3a, b, c). Taken together, the ABCA1 expression was consistently altered both in mRNA and protein level, which suggests that NNMT expression is associated with ABCA1 expression. Moreover, there were good linear relationships between their expressions both in mRNA and protein level in seven breast cancer cell lines (Supplementary Figs. 3d and e) and the IHC results of our cohort (Fig. 4d and e) which further suggested that there is a correlation between NNMT and ABCA1 expressions.

To confirm that NNMT reduces the intracellular cholesterol through cholesterol efflux, we detected the intracellular cholesterol level by inhibiting the synthesis and absorption of cholesterol. After pre-culturing in the complete media for 24 h, the cells were cultured in the medium with lipoprotein deficient serum and Mevastatin (HMG-CoA reductase inhibitor) for 8 h. The decrease in intracellular cholesterol in MDA-MB-231/NC cells was faster than those in MDA-MB-231/shNNMT-1 and MDA-MB-231/shNNMT-2 cells, whereas in HCC1937/Vector it was slower than that in HCC1937/NNMT<sup>OE</sup> (Fig. 4f), which suggested that NNMT reduces the intracellular cholesterol through enhancing cholesterol efflux.

Combined with these results, NNMT promotes ABCA1 expression to enhance the cholesterol efflux, leading to a decrease in cholesterol level in TNBC cells.

### 3.5. NNMT represses PP2A activity to activate MEK/ERK/c-Jun pathway thereby promoting ABCA1 expression in TNBC cells

c-Jun is a composed of transcription factor AP1, which is predicted to bind with ABCA1 promoter fragment to regulate ABCA1 expression at

transcription level [24]. We found that c-Jun protein was decreased after NNMT downregulation, whereas it was increased after NNMT overexpression (Fig. 5a). In addition, the c-Jun siRNA effectively knocked down the c-Jun expression and simultaneously decreased the ABCA1 protein and mRNA level (Fig. 5b and c). Furthermore, the relative light units of full-length ABCA1 promoter luciferase reporter showed a positive response induced by c-Jun plasmid in HEK 293T (Fig. 5d). These results indicated that c-Jun could regulate ABCA1 expression at transcription level in TNBC cells.

Further, we wondered whether NNMT could regulate c-Jun to promote ABCA1 expression in TNBC cells. We firstly detected the activation level of JNK and ERK pathways, where both regulate c-Jun transcription and activity. The phosphorylation level of ERK and c-Jun protein were decreased with NNMT knockdown in MDA-MB-231 cells, whereas p-ERK and c-Jun protein levels were increased with NNMT overexpression in HCC1937 cell, which were reversed by PD98059 (ERK activation inhibitor) (Fig. 5e and f). However, NNMT knockdown did not impair the JNK/c-Jun pathway in MDA-MB-231 cells (Supplementary Fig. 4). Taken together, these results indicate that NNMT increases ABCA1 expression by activating ERK/c-Jun pathway in TNBC cells. Moreover, c-Jun siRNA as well as ERK activation inhibitor could reverse the decrease of intracellular cholesterol level by NNMT expression. Moreover, the combination of c-Jun siRNA and ERK activation inhibitor could not increase intracellular cholesterol more than c-Jun siRNA or ERK activation inhibitor alone (Fig. 5g). These results indicated that NNMT mainly reduces intracellular cholesterol in TNBC cells by activating ERK/c-Jun pathway.

The activation of ERK pathway is mainly reflected in the phosphorylation of ERK by phosphorylated MEK. As one of the main serine/threonine phosphatases in mammalian cells [25], PP2A activity has been reported to be a key negative regulator of ERK pathway by affecting the phosphorylation of MEK [26]. PP2A activity is enhanced by methylation of the C-terminal Leu309 residue in its catalytic center [27], which was reported to be decreased by NNMT expression in cancer cells [3]. According to these reports, we detected the methylation level of PP2A and the phosphorylation level of MEK in our cell models. The results showed that the methylation level of PP2A was increased and the phosphorylation level of MEK was decreased with NNMT knockdown in MDA-MB-231 cells, whereas the methylated PP2A was decreased and the phosphorylated MEK was increased with NNMT overexpression in HCC1937 cells (Fig. 5h). These results indicated that NNMT attenuates the methylation level of PP2A to activate MEK/ERK pathway. To determine whether PP2A activity via Leu309 methylation indeed plays a critical role in NNMT-mediated TNBC metastasis, we exogenously added the PP2A inhibitor okadaic acid (OA) and PP2A activator perphenazine (PPZ) to the two cell models (MDA-MB-231 and HCC1937). As observed with downregulation of NNMT, there was an increase in the methylation of PP2A in the MDA-MB-231/NC cells upon the addition of PPZ. The cell mobility, invasiveness, and migration of MDA-MB-231/NC cells were attenuated by PPZ. In contrast, there was a decrease in the methylation of PP2A in the MDA-MB-231/shNNMT cells upon the addition of OA. Also, the cell mobility, invasiveness, and migration of MDA-MB-231/shNNMT cells were enhanced by OA (Fig. 5i and j).

Taken together, NNMT represses PP2A activity to activate MEK/ERK/c-Jun pathway leading to the increase in ABCA1 expression in TNBC cells.

### 3.6. NNMT promotes ABCA1 expression to reduce cholesterol leading to EMT

To determine the relationship between EMT and lowering cholesterol by NNMT, we detected the change of EMT-related molecules in our cell models. The EMT marker N-cadherin (CDH2), vimentin and EMT transcription factor Snail2 proteins were significantly decreased after NNMT downregulation, whereas the EMT marker E-cadherin protein (CDH1) was remarkably increased. Conversely, N-cadherin, vimentin

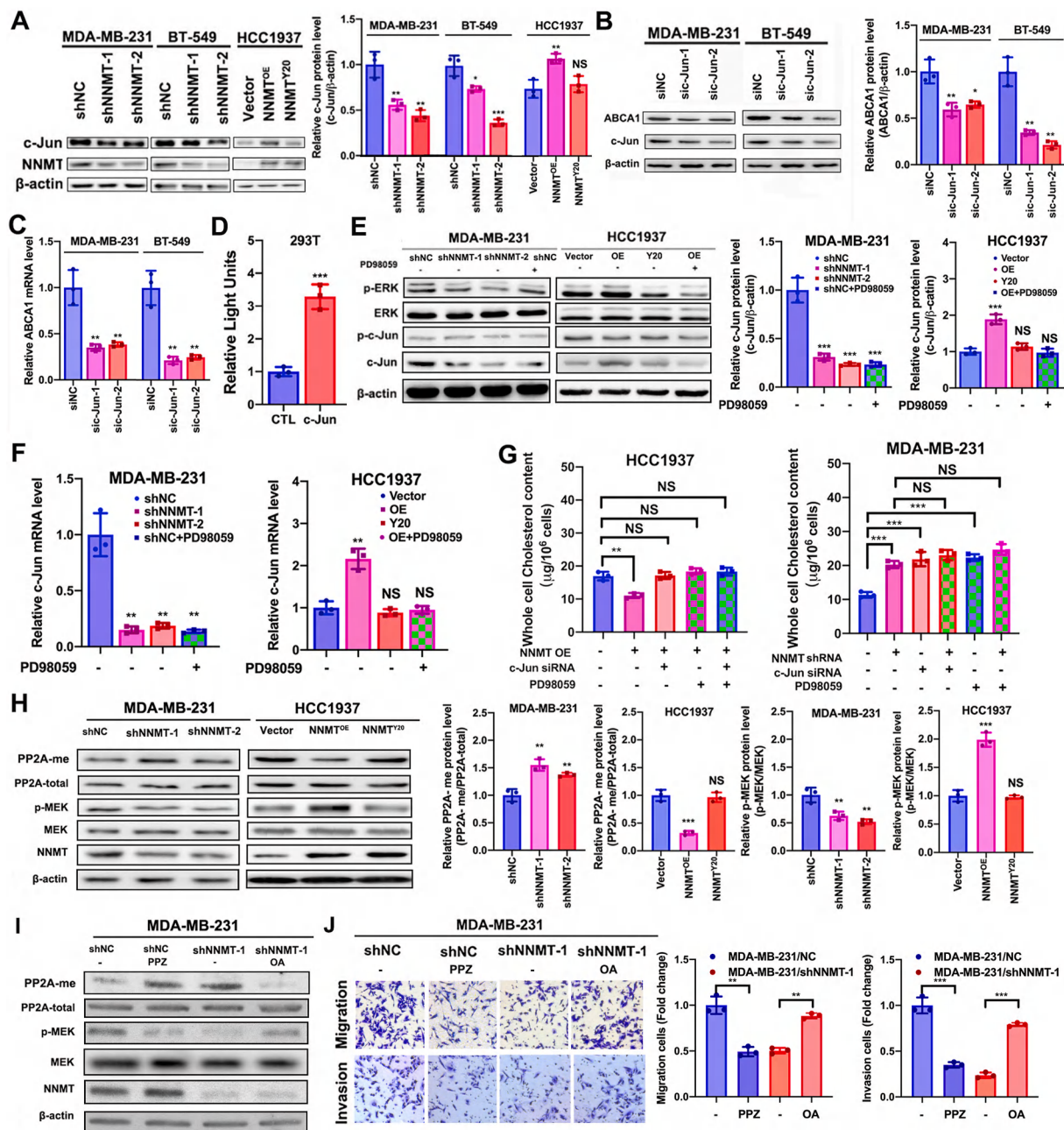


**Fig. 5.** NNMT represses PP2A activity to activate MEK/ERK/c-Jun pathway to promote ABCA1 expression in TNBC cells. (A) Representative result of c-Jun and NNMT proteins by western blotting in the cell models and quantification of relative c-Jun protein levels. (B) Representative result of c-Jun and ABCA1 proteins by western blotting and quantification of relative ABCA1 protein after c-Jun siRNA treatment. (C) Relative ABCA1 mRNA levels after c-Jun siRNA treatment. (D) ABCA1 promoter luciferase reporter signal of luciferase assay in HEK 293T cells. (E) Representative result of p-ERK, ERK, p-c-Jun and c-Jun protein by western blotting and quantification of relative c-Jun protein and mRNA levels (F) in MDA-MB-231 and HCC1937 cell models with or without PD98059 treatment. (G) Intracellular cholesterol levels with c-Jun siRNA or PD98059 treatment. (H) Representative result of methyl-PP2A, PP2A, p-MEK, MEK and NNMT proteins by western blotting and quantification of relative methyl-PP2A and p-MEK protein levels in MDA-MB-231 and HCC1937 cell models. (I) Representative result of methyl-PP2A, PP2A, p-MEK, MEK and NNMT proteins by western blotting in MDA-MB-231 cell model with PPZ or OA treatment. (J) Representative result of migration and invasion assays in MDA-MB-231 cell model with PPZ or OA treatment. Each experiment was repeated three times. Data are expressed as mean  $\pm$  SEM. (\* $P$  < 0.05, \*\* $P$  < 0.01, \*\*\* $P$  < 0.001, NS = not significant).

and Snail2 proteins were significantly increased after NNMT overexpression, whereas E-cadherin protein was remarkably decreased (Fig. 6a–g). Moreover, the same change happened in MDA-MB-231 cells with ABCA1 siRNA (Fig. 6h). The result of the analysis from Metabric dataset also showed that CDH2, vimentin and Snail2 were significantly upregulated in tumors with higher NNMT mRNA levels, which verifies our results (Fig. 6i). Taken together, these results indicated that NNMT promotes ABCA1 expression to reduce cholesterol leading to EMT.

### 3.7. NNMT knockdown inhibits the metastasis of TNBCs in vivo

To verify the function of NNMT on metastasis of TNBC *in vivo*, we constructed the mouse metastatic models of MDA-MB-231 and HCC1937 cells. The number of mice with metastasis (Supplementary Table 4) and the numbers of visible nodules and metastasis (Fig. 7a–d) in the lung of MDA-MB-231/shNNMT-1 group mice were all lower than those in the MDA-MB-231/shNC group, which suggested that NNMT

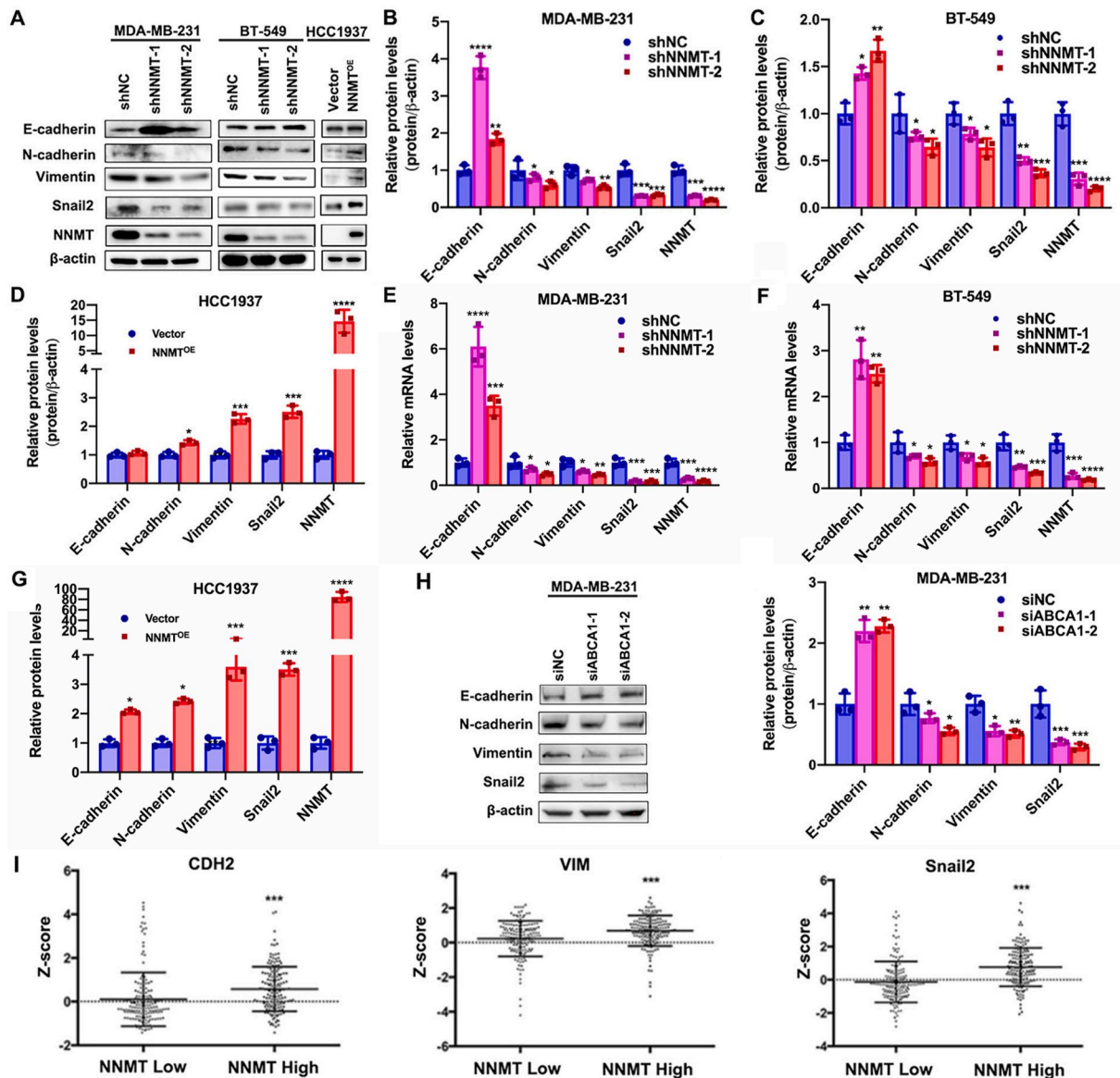


**Fig. 6.** NNMT promotes ABCA1 expression to reduce cholesterol leading to EMT. (A) Representative result of EMT related protein by western blotting. (B–D) Relative EMT related protein levels by western blotting. (E–G) Relative EMT related mRNA levels by qRT-PCR. (H) Representative result of EMT related protein by western blotting and quantification of relative EMT related protein levels in MDA-MB-231 cells with ABCA1 siRNA. (I) Relationship between CDH1, Vimentin, Snail2 and NNMT mRNA levels in Metabric dataset. Each experiment was repeated three times. Data are expressed as mean ± SEM. (\**P* < 0.05, \*\**P* < 0.01, \*\*\**P* < 0.001, \*\*\*\**P* < 0.0001).

downregulation inhibits the metastasis capacity of TNBC. In addition, NNMT, c-Jun and ABCA1 expressions were all decreased in the tumors of the MDA-MB-231/shNNMT-1 group compared with MDA-MB-231/shNC group by IHC analysis (Fig. 7e and f), which indicated that NNMT promotes the metastasis capacity of TNBC through increasing c-Jun regulated ABCA1 expression. In the HCC1937 cell mouse metastatic model, we only found metastasis in two mice with HCC1937/NNMT-WT cells not in mice with HCC1937/Vector or HCC1937/NNMT-Y20, which verified that NNMT expression increases the metastasis capacity of TNBC, and also implied that NNMT promotes the metastasis capacity by its catalytic function (Supplementary Fig. 5). Therefore, the results *in vivo* further demonstrated the critical promotion effect of NNMT on metastasis through increasing c-Jun regulated ABCA1 expression in TNBC metastasis.

Taken together, our result showed that NNMT is highly expressed in TNBC and associated with metastasis and survival by our cohort data and public datasets. In addition, NNMT repress PP2A activity to activate

MEK/ERK/c-Jun/ABCA1 pathway in TNBC cells, leading to the decrease of cholesterol and EMT activation, which finally enhances migration and invasion *in vitro* and metastasis capacity *in vivo*. Therefore, our findings suggested that NNMT is a link between cholesterol metabolism and metastasis in TNBC, which provides a new molecular mechanism to explain the high metastasis of TNBC.

#### 4. Discussion

Compared with other subtypes, TNBC had a higher metastasis rate and poor survival [28,29]. In addition, due to its special molecular phenotype, neither endocrine therapy nor molecular targeted therapy is suitable for TNBC treatment. Chemotherapy is the main treatment, but it cannot effectively overcome the metastasis, so the survival of TNBC is poor [30]. Therefore, it is necessary to delineate the mechanism of high metastasis in TNBC and develop a new treatment targeting metastasis to improve the survival of TNBC.

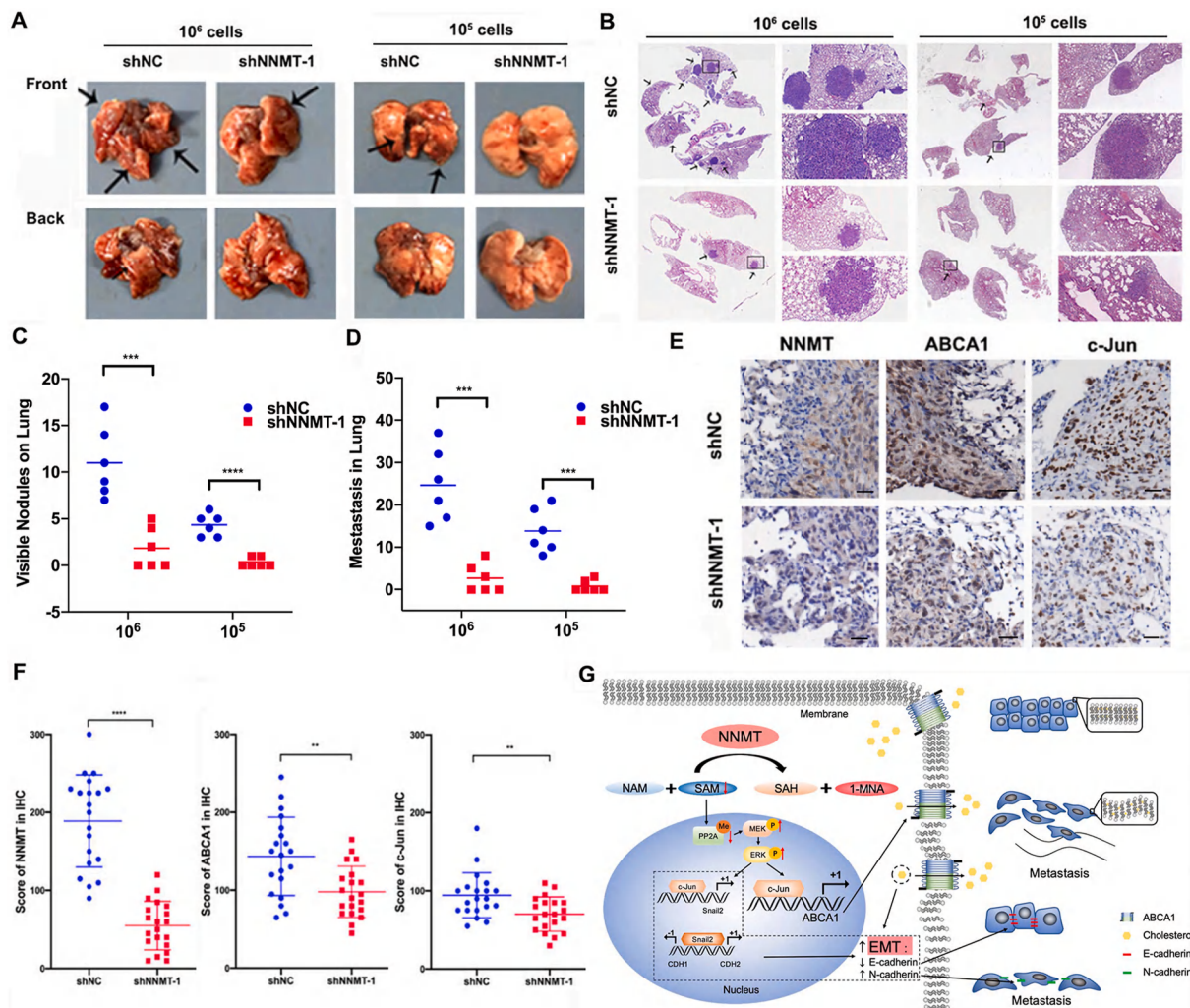


**Fig. 7.** NNMT promotes metastasis in the mouse metastatic models of MDA-MB-231 cells. (A) Lungs with visible nodules after injecting for  $10^6$  or  $10^5$  cells ( $n = 6$  for each group). (B) Representative result of H&E ( $\times 100$  and  $\times 400$ ) for metastasis in lungs. (C) Number of visible nodules on lungs for each mouse in two groups with  $10^6$  or  $10^5$  cells. (D) Number of metastasis in lungs for each mouse in two groups with  $10^6$  or  $10^5$  cells. (E) Representative result of NNMT, ABCA1 and c-Jun expressions in lungs in two groups with  $10^6$  cells by IHC (Scale bar: 100  $\mu\text{m}$ ). (F) Scores of NNMT, ABCA1 and c-Jun expressions in 20 random fields by IHC in lungs for each mouse in two groups with  $10^6$  cells. (G) Schematic model summarizes the promotion effect of NNMT/ERK/c-Jun/ABCA1 axis on high metastatic capacity of TNBC. (\*\* $P < 0.01$ , \*\*\* $P < 0.001$ , \*\*\*\* $P < 0.0001$ ).

NNMT transfers the methyl form SAM, an important methyl donor within cells, to NAM (the precursor of a large number of energy metabolism related molecules, such as NAD<sup>+</sup>, NADH), producing the stable metabolic product 1-MNA. Therefore, NNMT exerts specific control over the methylation potential and energy metabolism of cancer cells, where both impart a broad effect on the abnormal behavior of cancer cells, including sustaining proliferative signaling, evading growth suppressors, and resisting cell death [2]. NNMT was reported to promote cell proliferation in many types of cancer [12,17,31–33] and be a potential prognostic marker for some cancers [11,14–16]. Recently, we have reported that NNMT is highly expressed to enhance the chemoresistance in breast cancer [21]. Now, in this large patient observation data and public datasets (Metabric and TCGA), we found NNMT is particularly highly expressed in TNBC compared with other subtypes and plays an important role in the metastasis and survival of patients with TNBC. Moreover, NNMT expression significantly improves the metastasis capacity of the TNBC cell line HCC1937, which originally has low metastasis capacity, *in vitro* and *in vivo*. It seems to suggest that NNMT confers high metastasis capacity of TNBC. In addition, the TNBC cell line MDA-MB-231 and BT-549 with high metastasis capacity [34] have high NNMT expression, whereas the non-TNBC cell line MCF7, SK-BR-3,

T47D with low metastasis capacity have low or no NNMT expression (Supplementary Figs. 1a–c). In consistence with these reports, our results showed that the total intracellular cholesterol and SAM levels of MDA-MB-231 and BT-549 cell lines with high NNMT expression were lower than those of the other cell lines with low or no NNMT expression, whereas the 1-MNA level in MDA-MB-231 and BT-549 cell lines were higher than those of the other cell lines (Supplementary Figs. 6a–c). Furthermore, the cell mobility, invasiveness, migration, c-Jun and MEK/ERK signaling levels of MDA-MB-231 and BT-549 cell lines were higher than those of the other cell lines (Supplementary Figs. 6d–h), which indicated that NNMT played some general roles in metastasis of breast cancer.

EMT is generally considered to be a major driver of metastasis [35]. The increased membrane fluidity also is a necessary cellular feature of metastatic potential, which is decided by the cholesterol on the cell membrane [23,36]. We determined that NNMT reduces the cholesterol level in cytoplasm and on cell membrane in TNBCs by inducing ABCA1 expression to enhance cholesterol efflux. Moreover, we confirmed the prediction that c-Jun may be a transcription factor of ABCA1 through binding AP1 on the promoter of ABCA1 [24] and also may explain the report that ABCA1 was overexpressed in 41% of patients with metastatic

breast cancer and reduced time to metastasis by nine years in four public datasets [23], which demonstrates that high NNMT induces ABCA1 expression to enhance cholesterol efflux by EKR/c-Jun pathway, leading to metastasis enhancement. Besides, in breast cancer cells, we have reported that NNMT activates ERK pathway [20], which was reported to increase c-Jun transcription and stability. Moreover, the EMT related transcription factors were found to be regulated by upstream transcription factors or signaling pathways, such as c-Jun [37]. The inhibition of c-Jun/Snail2 axis suppresses the EMT of lung cancer [38], which is consistent with our results. Based on our results and these reports, we believe that NNMT promotes metastasis capacity of TNBC by activating ERK/c-Jun pathway to induce EMT and regulating cholesterol metabolism to enhance membrane fluidity.

On the mechanism for activating the EKR/c-Jun pathway by NNMT, we confirmed that NNMT reduces the methylation level of PP2A in TNBCs, which is **consistent** with the previous reports in other cancers [3,39,40]. PP2A is a de-phosphorylase of serine/threonine. Methylation of the C-terminal leucine residue (Leu-309) of PP2A-C allows for the assembly and activation of the PP2A trimer. The methylation is reversibly controlled by a PP2A-specific methyltransferase known as leucine carboxyl methyl transferase 1 (LCMT1) and by PP2A-specific methyl esterase 1 (PME-1) [41]. In glioblastoma, it is reported that NNMT outcompetes LCMT1 for methyl transfer from principal methyl donor SAM in cancer cells. The knockdown of NNMT increased the availability of methyl groups for LCMT1 to methylate PP2A, resulting in the inhibition of oncogenic serine/threonine kinases (STK) [39]. PP2A has been reported to dephosphorylate over 300 substrates due to the diversity of its holoenzyme structure. Recently, NNMT was reported to repress PP2A activity to activate AKT (Ser473/Thr308) and MEK (Ser217/221) in glioblastoma [39] as well as ULK1 (Ser638) [40] in liver cancer. These results suggest that NNMT could modulate other signaling pathways with serine/threonine phosphorylation sites through PP2A, thereby performing specific functions in cancers. In addition, the consumption of SAM by NNMT not only impairs the methylation of PP2A, but also the methylation of histones, thus directly affecting the transcriptional expression of oncogenes and tumor suppressor genes, including Snail2, TGFB2, CNTN1, ADAMTS6 and LAMB3 [3]. In our study, we also found that NNMT expression promotes Snail2, leading to EMT (Fig. 6a–g). However, we further found that ABCA1 and c-Jun siRNA both can inhibit the Snail2 expression to reverse the EMT by NNMT overexpression in TNBCs (Fig. 6h and Supplementary Fig. 7). These results indicate that NNMT regulates the Snail2 expression in different ways. According to previous studies, NNMT was believed to be involved in the regulation of a wide range of metabolic pathways, including glucose, lipid and cholesterol metabolism in liver and lipid metabolism in cancer cells [3,19,42]. Our study linked the basic methyl transfer function of NNMT to its involvement in metabolism and functioning in TNBCs.

Zhao et al. reported that the repressed cholesterol by CtBP protein activates TGF- $\beta$  signaling and EMT to promote metastasis of breast cancer [43]. In addition, the increased cholesterol efflux enhances membrane fluidity of breast cancer cells, resulting in cell motility and EMT *in vitro* and metastasis *in vivo* [23]. These reports indicate that cholesterol also can negatively regulate EMT to enhance metastasis capacity of cancer cells, which is consistent with our results. Therefore, our finding suggests that cholesterol is a protective factor for metastasis in breast cancer at cancer cell line level. A range of retrospective clinical studies have addressed the risk of metastasis in breast cancer by cholesterol, mainly focusing on serum cholesterol. However, these studies had equivocal results, with most finding that cholesterol is not associated with breast metastasis, some indicating a protective effect of cholesterol, while others implicating cholesterol as a significant risk factor [44]. Therefore, the correlation between cholesterol level and the risk of metastasis in patients with breast cancer is controversial and requires more in-depth research.

In summary, we found that NNMT reduces the cholesterol level in the

cytoplasm and on cell membrane to enhance membrane fluidity of TNBCs by repressing PP2A activity to activate MEK/ERK/c-Jun/ABCA1, leading to EMT activation. Based on these findings, we made a hypothetical schematic (Fig. 7g). Our study provides a new molecular mechanism to explain the high metastasis of TNBC and suggests that NNMT could be regarded as a potential/promising target for the treatment of breast cancer in the future.

#### Availability of data and material

All datasets used and/or analyzed during the current study are available from the corresponding author on reasonable request.

#### CRediT authorship contribution statement

**Yanzhong Wang:** Validation, Formal analysis, Writing – review & editing, Funding acquisition. **Xi Zhou:** Investigation, Writing – original draft. **Yinjiao Lei:** Investigation, Formal analysis. **Yadong Chu:** Investigation, Formal analysis. **Xingtong Yu:** Investigation, Formal analysis. **Qingchao Tong:** Investigation, Data curation. **Tao Zhu:** Methodology. **Haitao Yu:** Investigation, Data curation. **Sining Fang:** Investigation, Data curation. **Guoli Li:** Investigation, Data curation. **Linbo Wang:** Writing – review & editing, Validation. **Gavin Y. Wang:** Writing – review & editing, Validation. **Xinyou Xie:** Supervision, Project administration. **Jun Zhang:** Conceptualization, Visualization, Funding acquisition.

#### Declaration of competing interest

The authors declare that they have no competing interests.

#### Acknowledgements

This work was supported by the National Natural Science Foundation of China (No:82172362), Key Program of Zhejiang Provincial Traditional Chinese Medicine Foundation (No:2018ZZ016), Key Research and Development Program of Zhejiang Province (No:2019C03021), Natural Science Foundation of Zhejiang Province (No:LQ20H200004), and Zhejiang Provincial Health Bureau Foundation (No:2020RC021). Key Laboratory of Precision Medicine in Diagnosis and Monitoring Research of Zhejiang Province (No:2022E10018).

#### Appendix A. Supplementary data

Supplementary data to this article can be found online at <https://doi.org/10.1016/j.canlet.2022.215884>.

#### References

- [1] L. Yin, J.J. Duan, X.W. Bian, S.C. Yu, Triple-negative breast cancer molecular subtyping and treatment progress, *Breast Cancer Res.* 22 (2020) 61.
- [2] D. Hanahan, Hallmarks of cancer: new dimensions, *Cancer Discov.* 12 (2022) 31–46.
- [3] O.A. Ulanovskaya, A.M. Zuhl, B.F. Cravatt, NNMT promotes epigenetic remodeling in cancer by creating a metabolic methylation sink, *Nat. Chem. Biol.* 9 (2013) 300–306.
- [4] J.M. Markert, C.M. Fuller, G.Y. Gillespie, J.K. Buben, L.A. McLean, R.L. Hong, K. Lee, S.R. Gullans, T.B. Mapstone, D.J. Benos, Differential gene expression profiling in human brain tumors, *Physiol. Genom.* 5 (2001) 21–33.
- [5] J. Xu, F. Moatamed, J.S. Caldwell, J.R. Walker, Z. Kraiem, K. Taki, G.A. Brent, J. M. Hershman, Enhanced expression of nicotinamide N-methyltransferase in human papillary thyroid carcinoma cells, *J. Clin. Endocrinol. Metab.* 88 (2003) 4990–4996.
- [6] J.S. Jang, H.Y. Cho, Y.J. Lee, W.S. Ha, H.W. Kim, The differential proteome profile of stomach cancer: identification of the biomarker candidates, *Oncol. Res.* 14 (2004) 491–499.
- [7] M. Roessler, W. Rollinger, S. Palme, M.L. Hagmann, P. Berndt, A.M. Engel, B. Schneidinger, M. Pfeffer, H. Andres, J. Karl, H. Bodenmuller, J. Ruschoff, T. Henkel, G. Rohr, S. Rossol, W. Rosch, H. Langen, W. Zolg, M. Tacke, Identification of nicotinamide N-methyltransferase as a novel serum tumor marker for colorectal cancer, *Clin. Cancer Res.* 11 (2005) 6550–6557.

- [8] M. Yao, H. Tabuchi, Y. Nagashima, M. Baba, N. Nakaigawa, H. Ishiguro, K. Hamada, Y. Inayama, T. Kishida, K. Hattori, H. Yamada-Okabe, Y. Kubota, Gene expression analysis of renal carcinoma: adipose differentiation-related protein as a potential diagnostic and prognostic biomarker for clear-cell renal carcinoma, *J. Pathol.* 205 (2005) 377–387.
- [9] B.H. Lim, B.I. Cho, Y.N. Kim, J.W. Kim, S.T. Park, C.W. Lee, Overexpression of nicotinamide N-methyltransferase in gastric cancer tissues and its potential post-translational modification, *Exp. Mol. Med.* 38 (2006) 455–465.
- [10] D. Sartini, A. Santarelli, V. Rossi, G. Goteri, C. Rubini, D. Ciavarella, L. Lo Muzio, M. Emanuelli, Nicotinamide N-methyltransferase upregulation inversely correlates with lymph node metastasis in oral squamous cell carcinoma, *Mol. Med.* 13 (2007) 415–421.
- [11] J. Kim, S.J. Hong, E.K. Lim, Y.S. Yu, S.W. Kim, J.H. Roh, I.G. Do, J.W. Joh, D. S. Kim, Expression of nicotinamide N-methyltransferase in hepatocellular carcinoma is associated with poor prognosis, *J. Exp. Clin. Cancer Res.* 28 (2009) 20.
- [12] V. Pozzi, D. Sartini, S. Morganti, R. Giuliani, G. Di Ruscio, A. Santarelli, R. Rocchetti, C. Rubini, M. Tomasetti, G. Giannatempo, F. Orlando, M. Provinciali, L. Lo Muzio, M. Emanuelli, RNA-mediated gene silencing of nicotinamide N-methyltransferase is associated with decreased tumorigenicity in human oral carcinoma cells, *PLoS One* 8 (2013), e71272.
- [13] M.G. Thomas, M. Saldanha, R.J. Mistry, D.T. Dexter, D.B. Ramsden, R.B. Parsons, Nicotinamide N-methyltransferase expression in SH-SY5Y neuroblastoma and N27 mesencephalic neurones induces changes in cell morphology via ephrin-B2 and Akt signalling, *Cell Death Dis.* 4 (2013) e669.
- [14] W. Zhou, M. Gui, M. Zhu, Z. Long, L. Huang, J. Zhou, L. He, K. Zhong, Nicotinamide N-methyltransferase is overexpressed in prostate cancer and correlates with prolonged progression-free and overall survival times, *Oncol. Lett.* 8 (2014) 1175–1180.
- [15] C. Chen, X. Wang, X. Huang, H. Yong, J. Shen, Q. Tang, J. Zhu, J. Ni, Z. Feng, Nicotinamide N-methyltransferase: a potential biomarker for worse prognosis in gastric carcinoma, *Am. J. Cancer Res.* 6 (2016) 649–663.
- [16] Y. Xu, P. Liu, D.H. Zheng, N. Wu, L. Zhu, C. Xing, J. Zhu, Expression profile and prognostic value of NNMT in patients with pancreatic cancer, *Oncotarget* 7 (2016) 19975–19981.
- [17] Y. Wu, M.S. Siadaty, M.E. Berens, G.M. Hampton, D. Theodorescu, Overlapping gene expression profiles of cell migration and tumor invasion in human bladder cancer identify metallothionein 1E and nicotinamide N-methyltransferase as novel regulators of cell migration, *Oncogene* 27 (2008) 6679–6689.
- [18] R.B. Parsons, S. Aravindan, A. Kadampeswaran, E.A. Evans, K.K. Sandhu, E. R. Levy, M.G. Thomas, B.M. Austen, D.B. Ramsden, The expression of nicotinamide N-methyltransferase increases ATP synthesis and protects SH-SY5Y neuroblastoma cells against the toxicity of Complex I inhibitors, *Biochem. J.* 436 (2011) 145–155.
- [19] S. Hong, J.M. Moreno-Navarrete, X. Wei, Y. Kikukawa, I. Tzamelis, D. Prasad, Y. Lee, J.M. Asara, J.M. Fernandez-Real, E. Maratos-Flier, P. Pissios, Nicotinamide N-methyltransferase regulates hepatic nutrient metabolism through Sirt1 protein stabilization, *Nat. Med.* 21 (2015) 887–894.
- [20] J. Zhang, Y. Wang, G. Li, H. Yu, X. Xie, Down-regulation of nicotinamide N-methyltransferase induces apoptosis in human breast cancer cells via the mitochondria-mediated pathway, *PLoS One* 9 (2014), e89202.
- [21] Y. Wang, J. Zeng, W. Wu, S. Xie, H. Yu, G. Li, T. Zhu, F. Li, J. Lu, G.Y. Wang, X. Xie, J. Zhang, Nicotinamide N-methyltransferase enhances chemoresistance in breast cancer through SIRT1 protein stabilization, *Breast Cancer Res.* 21 (2019) 64.
- [22] R.M. Neve, K. Chin, J. Fridlyand, J. Yeh, F.L. Baehner, T. Fevr, L. Clark, N. Bayani, J.P. Coppe, F. Tong, T. Speed, P.T. Spellman, S. DeVries, A. Lapuk, N.J. Wang, W. L. Kuo, J.L. Stilwell, D. Pinkel, D.G. Albertson, F.M. Waldman, F. McCormick, R. B. Dickson, M.D. Johnson, M. Lippman, S. Ethier, A. Gazdar, J.W. Gray, A collection of breast cancer cell lines for the study of functionally distinct cancer subtypes, *Cancer Cell* 10 (2006) 515–527.
- [23] W. Zhao, S. Prijic, B.C. Urban, M.J. Tisza, Y. Zuo, L. Li, Z. Tan, X. Chen, S.A. Mani, J.T. Chang, Candidate antimetastasis drugs suppress the metastatic capacity of breast cancer cells by reducing membrane fluidity, *Cancer Res.* 76 (2016) 2037–2049.
- [24] S. Santamarina-Fojo, K. Peterson, C. Knapper, Y. Qiu, L. Freeman, J.F. Cheng, J. Osorio, A. Remaley, X.P. Yang, C. Haudenschild, C. Prades, G. Chimini, E. Blackmon, T. Francois, N. Duverger, E.M. Rubin, M. Rosier, P. Deneffe, D. S. Fredrickson, H.B. Brewer Jr., Complete genomic sequence of the human ABCA1 gene: analysis of the human and mouse ATP-binding cassette A promoter, *Proc. Natl. Acad. Sci. U. S. A.* 97 (2000) 7987–7992.
- [25] D. Perrotti, P. Neviani, Protein phosphatase 2A: a target for anticancer therapy, *Lancet Oncol.* 14 (2013) e229–238.
- [26] M.R. Junttila, S.P. Li, J. Westermarck, Phosphatase-mediated crosstalk between MAPK signaling pathways in the regulation of cell survival, *Faseb. J.* 22 (2008) 954–965.
- [27] P.J. Eichhorn, M.P. Creighton, R. Bernards, Protein phosphatase 2A regulatory subunits and cancer, *Biochim. Biophys. Acta* 1795 (2009) 1–15.
- [28] A.G. Waks, E.P. Winer, Breast cancer treatment: a review, *JAMA* 321 (2019) 288–300.
- [29] A. Lee, M.B.A. Djamgoz, Triple negative breast cancer: emerging therapeutic modalities and novel combination therapies, *Cancer Treat Rev.* 62 (2018) 110–122.
- [30] M.G. Ferraro, M. Piccolo, G. Misso, F. Maione, D. Montesarchio, M. Caraglia, L. Paduano, R. Santamaria, C. Irace, Breast cancer chemotherapeutic options: a general overview on the preclinical validation of a multi-target ruthenium(III) complex lodged in nucleolipid nanosystems, *Cells* 9 (2020).
- [31] T. Yu, Y.T. Wang, P. Chen, Y.H. Li, Y.X. Chen, H. Zeng, A.M. Yu, M. Huang, H.C. Bi, Effects of nicotinamide N-methyltransferase on PANC-1 cells proliferation, metastatic potential and survival under metabolic stress, *Cell. Physiol. Biochem.* 35 (2015) 710–721.
- [32] S.W. Tang, T.C. Yang, W.C. Lin, W.H. Chang, C.C. Wang, M.K. Lai, J.Y. Lin, Nicotinamide N-methyltransferase induces cellular invasion through activating matrix metalloproteinase-2 expression in clear cell renal cell carcinoma cells, *Carcinogenesis* 32 (2011) 138–145.
- [33] X. Xie, H. Yu, Y. Wang, Y. Zhou, G. Li, Z. Ruan, F. Li, X. Wang, H. Liu, J. Zhang, Nicotinamide N-methyltransferase enhances the capacity of tumorigenesis associated with the promotion of cell cycle progression in human colorectal cancer cells, *Arch. Biochem. Biophys.* 564 (2014) 52–66.
- [34] K. Spring, P. Fournier, L. Lapointe, C. Chabot, J. Roussy, S. Pommey, J. Stagg, I. Royal, The protein tyrosine phosphatase DEP-1/PTPRJ promotes breast cancer cell invasion and metastasis, *Oncogene* 34 (2015) 5536–5547.
- [35] L.J. Fidler, The pathogenesis of cancer metastasis: the 'seed and soil' hypothesis revisited, *Nat. Rev. Cancer* 3 (2003) 453–458.
- [36] Z. Yang, W. Qin, Y. Chen, B. Yuan, X. Song, B. Wang, F. Shen, J. Fu, H. Wang, Cholesterol inhibits hepatocellular carcinoma invasion and metastasis by promoting CD44 localization in lipid rafts, *Cancer Lett.* 429 (2018) 66–77.
- [37] Q. Meng, Y. Xia, c-Jun, at the crossroad of the signaling network, *Protein Cell* 2 (2011) 889–898.
- [38] J.Y. Shih, M.F. Tsai, T.H. Chang, Y.L. Chang, A. Yuan, C.J. Yu, S.B. Lin, G.Y. Liou, M.L. Lee, J.J. Chen, T.M. Hong, S.C. Yang, J.L. Su, Y.C. Lee, P.C. Yang, Transcription repressor slug promotes carcinoma invasion and predicts outcome of patients with lung adenocarcinoma, *Clin. Cancer Res.* 11 (2005) 8070–8078.
- [39] K. Palanichamy, S. Kanji, N. Gordon, K. Thirumoorthy, J.R. Jacob, K.T. Litzenberg, D. Patel, A. Chakravarti, NNMT silencing activates tumor suppressor PP2A, inactivates oncogenic STKs, and inhibits tumor forming ability, *Clin. Cancer Res.* 23 (2017) 2325–2334.
- [40] J.H. Shin, C.W. Park, G. Yoon, S.M. Hong, K.Y. Choi, NNMT depletion contributes to liver cancer cell survival by enhancing autophagy under nutrient starvation, *Oncogenesis* 7 (2018) 58.
- [41] Y. Xing, Z. Li, Y. Chen, J.B. Stock, P.D. Jeffrey, Y. Shi, Structural mechanism of demethylation and inactivation of protein phosphatase 2A, *Cell* 133 (2008) 154–163.
- [42] P. Pissios, Nicotinamide N-methyltransferase: more than a vitamin B3 clearance enzyme, *Trends Endocrinol. Metab.* 28 (2017) 340–353.
- [43] Z. Zhao, D. Hao, L. Wang, J. Li, Y. Meng, P. Li, Y. Wang, C. Zhang, H. Zhou, K. Gardner, L.J. Di, CtBP promotes metastasis of breast cancer through repressing cholesterol and activating TGF-beta signaling, *Oncogene* 38 (2019) 2076–2091.
- [44] E.R. Nelson, C.Y. Chang, D.P. McDonnell, Cholesterol and breast cancer pathophysiology, *Trends Endocrinol. Metab.* 25 (2014) 649–655.